JOURNAL OF OPTOELECTRONICS AND ADVANCED MATERIALS Vol. 9, No. 5, May 2007, p. 1478 - 1491

Review Paper

Nanostructured magnetic materials obtained by mechanical alloying/milling

V. POP*, I. CHICINAŞ[a]
Faculty of Physics, Babes-Bolyai University, 4000480 Cluj-Napoca, Romania
[a]Materials Sciences and Technology Dept., Technical University of Cluj-Napoca, 103-105 Muncii ave., 400641 Cluj-Napoca, Romania

Generally, polycrystalline solids with grain size less than 100 nm are called nanocrystalline materials. Nanomaterials behave differently from their macroscopic counterparts because their characteristic sizes are smaller than the characteristic length scales of physical phenomena occurring in bulk materials. Nanocrystalline structures offer a new opportunity to improve current magnetic materials. This refers to materials such as permanent magnets, soft magnetic materials, recording media and also to materials involved in spin electronics. The properties of nanocrystalline materials are very often superior to those of conventional polycrystalline coarse grain materials. These materials can be produced using various methods and different starting phases: vapour (inert gas condensation, sputtering, plasma processing, vapour deposition), liquid (electrodeposition, rapid solidification) or solid (mechanical alloying, severe plastic deformation, spark erosion). A survey on mechanical alloying and mechanical milling as methods to obtain nanostructured permanent magnets and soft magnetic materials will be presented. The influence of the annealing on the structure and microstructure is also discussed. Some of our results obtained in soft Ni-Fe based magnetic materials and in spring magnets type materials, obtained by mechanical alloying (soft magnetic materials) or by mechanical milling (spring magnets) and annealing, are presented.

(Received November 14, 2006; accepted April 12, 2007)

Keywords: Soft magnetic materials, Spring magnets, Mechanical alloying/milling

1. Introduction

Nanocrystalline ferromagnetic materials exhibit magnetic properties which are interesting both from a fundamental research of magnetism as well as for applications. They play an important role in the field of new soft and hard magnetic materials [1-5].

In hard-magnetic materials, exchange coupling between the nano-sized grains causes a remanence enhancement, which means that even in isotropic materials a remanence M_r of more than 50% of the saturation magnetization M_s can be achieved. An example of improving the performance of hard magnetic materials by nanostructuring is *hard-soft* permanent magnet composites known as *exchange-spring magnets* [3, 6-13]. Exchange-spring magnets or spring magnets consist of nanodispersed hard and soft magnetic phases that are coupled by exchange. Spring magnets combine the high anisotropy of the hard phases with the large magnetisation found in soft magnetic phases. There are two basic parameters that characterise the structure of the nanostructured materials: the crystallites diameter, D, and the volume fraction of the nanocrystalline phases, V_{cr}. In hard magnetic nanocrystalline materials full or almost full crystallization is required. The critical dimension for the soft phase, below which the soft phase is rigidly coupled to the hard phase, is found to be roughly twice the width of domain wall in the hard phase, $\delta_h = \pi\sqrt{A_h / K_h}$ [14], where A_h and K_h are the exchange and anisotropy constants [15] of the hard phase, respectively. From experimental point of view, a large reversible demagnetization curve in conjunction with a strength remanence, $m_r > 0.5$ ($m_r = M_r/M_s$), may be considered a criteria for the presence of the exchange spring mechanism.

Nanocrystalline soft-magnetic materials leads both to a higher permeability and a reduced coercivity, and consequently to lower losses [5, 16]. Amorphous and nanocrystalline soft magnetic materials applications can be found in many types of industrial products which include transformers, motors, sensors, power electronics, electrical energy control/management systems, telecommunication equipment and pulse power devices [17]. The wide range of applications arises from the versatile nature of these materials which can provide fast magnetization reversal with minimal magnetic losses. Sometimes nanocrystalline soft magnetic materials can be designed for specific applications. In developing a soft magnetic material, two main aspects are of interest from an application point of view: (1) materials with as high permeability as possible and (2) materials with the saturation induction B_s as high as possible. Also for ac applications the materials is preferably to have as high resistivity as possible. Co-based amorphous alloys with permeabilities reaching of 10^6 have been obtained, but the upper limit for B_s is about 1 T.

Fe-based amorphous alloys can reach $B_s \approx 1.8$ T [2]. Generally, the optimum mechanical and magnetic properties of the nanocrystalline soft magnetic materials are obtained for partial crystallisation materials. This means that these materials are two-phase: a nanocrystalline and an amorphous matrix [18]. The volume fraction of the nanocrystalline phase should follow the criteria that its negative magnetostriction contribution compensates the positive magnetostriction contribution of the amorphous matrix. In the non-magnetostrictive iron nanocrystalline materials $V_{cr} \approx 70$-75 % depending on alloy composition. The nanocrystallite diameter, D, should be smaller than the magnetic exchange length, $L_{ex} = \sqrt{A / K_1}$, in the crystalline phase to reduce the magnetocrystalline anisotropy of this phase. According with the random anisotropy model [16] D should be smaller than 15 nm for α-Fe(Si) and α-Fe nanocrystals present in Finemet ($Fe_{73.5}Cu_1Nb_3Si_{13.5}B_9$) and Nanoperm ($Fe_{84}Zr_{3.5}Nb_{3.5}B_8Cu_1$) alloys, respectively. Typical values for the exchange length are 5-10 nm for Co-based alloys and 20-40 nm for Fe-based alloys [19]. In classical crystalline soft materials it is well known that the coercivity increases by decreasing grain size ($1/D$ dependence); good soft magnetic properties require very large grains, $D > 100$ μm. Thus, the reduction of particle size to the regime of the domain wall width increases coercive field, H_c, toward a maximum given by the material anisotropy; fine particle system been compatible as hard magnetic materials. In the nanoscale region this behaviour changes. A critical grain size, D_{cr} (of about 40 nm), which divides the $H_c(D)$ behaviour in two different regions can be observed [16,19]. The crystallite refinement ($D<D_{cr}$) reduces the magnetocrystalline anisotropy due to the averaging effect of magnetisation over randomly oriented nanocrystallites, leading also to a reduction of H_c. Fig. 1 summarises the $H_c(D)$ behaviour in the whole range of structural correlation lengths from atomic distances in amorphous alloys up to macroscopic grain size [20]. The magnetic permeability shows an analogous behaviour, being essentially proportional to $1/H_c$. The D^6 dependence of H_c in the nanometric region ($D < D_{cr}$, Fig. 1) shows how closely hard and soft magnetic behaviour can be neighboured and decided by the correlation between grain size and ferromagnetic exchange length. Contrary to the fact that the vanish of the coercivity in superparamagnetic regime is accompanied by a low permeability, in the soft magnetic nanostructures small ferromagnetic crystallites are well coupled by exchange interactions and have simultaneously low coercivity and high permeability.The deviations from the theoretical D^6 dependence could be explained by the presence of the additional crystalline phases and/or magneto-elastic and induced anisotropies. When the exchange interactions starts to dominate over anisotropy, $D<D_{cr}$, the remanence enhancements towards 1, $J_r/J_s \rightarrow 1$. If $D<<D_{cr}$ the remanence ratio decrease to a value around 0.5 [5]. Nanocrystalline materials exhibit increased strength/hardness, reduced density, reduced elastic modulus, smaller electrical conductivity, higher specific heat, higher thermal expansion coefficient, lover thermal conductivity, and better soft magnetic properties in comparison with polycrystalline coarse grain materials.

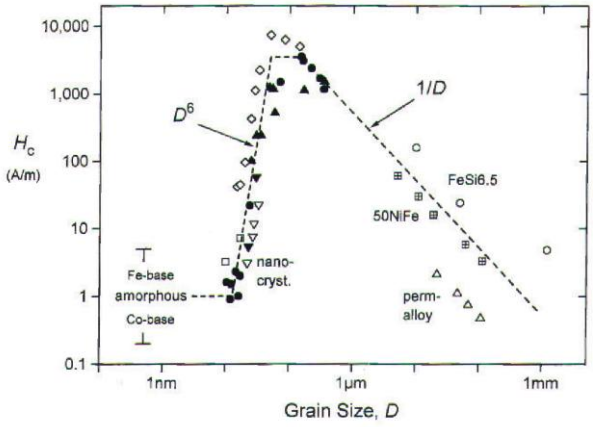

Fig. 1. Coercive field, H_c, vs. grain size, D, for various soft magnetic alloys: ▲ Fe-Nb-Si-B, ● Fe-Cu-Nb-Si-B, ▼▽ Fe-Cu-V-Si-B, □ Fe-Zr-B, ◊ Fe-Co-Zr, △ NiFe and ○ Fe-Si(6.5 %). Reprinted from [20], Copyright (1997), with permission from Elsevier.

Mechanical alloying, MA, and mechanical milling, MM, involves the synthesis of materials by high-energy ball milling in planetary mills, vibratory mills, attritors and tumbling ball mills. For MA and MM, the weight rate powder/balls is usually from 1/7 to 1/10, but can be found also rates up to 1/20. Mechanical alloying allows producing nonequilibrium structure/microstructure including amorphous alloys, extended solid solutions, metastable crystalline phases, nanocrystalline materials and quasi crystals [11, 21-27]. Materials obtained by mechanical alloying or mechanical milling present an unusual distribution of structural defects compared with those prepared by traditional methods. As a consequence of the high number of crystalline defects it is possible to obtain amorphous alloys by mechanical alloying even for a negative energy for amorphous phase formation [21, 28]. The materials obtained by mechanical alloying or mechanical milling form metastable phases. The importance of the metastable phases for the magnetic materials applications is one of the motivations for the extensive investigations of the nanostructured materials. The optimisation of the microstructure is the key to improve the hard magnetic properties of nanocrystalline soft magnetic materials as well as nanocomposite permanent magnets. Mechanical milling/alloying combined with appropriate heat treatments for microstructure refinement was frequently used to obtain

nanocomposite hard magnetic materials or nanocrystalline soft magnetic materials.

2. Soft magnetic nanocrystalline materials obtained by mechanical alloying

Nanocrystalline soft magnetic materials obtained by mechanical alloying/milling present the advantage of an enforced resistivity (important in ac applications), but the significant density of defects can increase the coercivity. Consequently, the fabrication of nanocrystalline soft magnetic materials by MA implies more care than other techniques. In last two decades, the various mechanical routes (mechanical alloying, mechanical milling, reactive milling (RM), mechanical alloying combined with annealing and their technological variants) were used in producing soft magnetic nanocrystalline powders (ferrites and alloys). An overview on the soft magnetic nanocrystalline materials produced by mechanical routes is presented in [29].

The nanocrystalline/nanosized ferrites were prepared especially by two basically mechanical routes: (i) directly, by reactive milling of oxides or others precursor's mixture [30-37] and (ii) by dry or wet milling of the polycrystalline ferrites obtained by classical methods [30, 33, 38-49]. As type of ferrites, by mechanical routes were obtained the follows: Fe_3O_4 [50, 51], $NiFe_2O_4$ [31-33, 40, 41, 52, 53], $CuFe_2O_4$ [30, 38, 39], $ZnFe_2O_4$ [33, 34, 42- 44, 54, 55], $MnFe_2O_4$ [36, 56], $MgFe_2O_4$ [35, 45-47,52, 57], $CoFe_2O_4$ [37, 58], $CdFe_2O_4$ [48, 49], $NiAlFeO_4$ [59], $Mn_{(1-x)}Zn_xFe_2O_4$ [60].

Generally, in the case of the soft magnetic ferrites produced by mechanical routes, a partial reversibility during milling of the reaction $\alpha\text{-}Fe_2O_3 + MeO \leftrightarrow MeFe_2O_4$ was evidenced and the particles contain several related Fe–Me–O phases. This behaviour was observed in many systems, like Fe-Cu-O [30, 38, 39], Fe-Mn-O [36], Fe-Ni-O [33] or Fe-Zn-O [54]. As a consequence of the partial reversibility of the reaction, the complete formation of $ZnFe_2O_4$ spinel phase was obtained after 1320 hours of milling, while the $CuFe_2O_4$ phase cannot be obtained by RM even for milling times as long as 1600 hours [54]. The $ZnFe_2O_4$ spinel phase was obtained in all volume of the sample by RM of 1:1 molar mixture of α-Fe_2O_3 and ZnO after 623 hours of milling and 1 h of annealing at 227 °C [35].

The soft magnetic nanocrystalline/nanosized ferrites produced by mechanical routes present also particle size with a superparamagnetic (SPM) behaviour [40, 41, 44, 50, 51, 53, 55] and a spin canted effect [32, 33, 38, 40, 42, 46, 48, 49, 54]. Also, a cation redistribution between A and B sites was observed [30, 32, 38]. As a consequence of the spin canted magnetic structures, a nonsaturated magnetisation (even at a field of 9 T [38]) and a ΔH_C shift to the left, depending on the milling time, were reported [38, 39, 46]. A decrease of the Curie temperature with increasing the milling time was observed for the $MgFe_2O_4$ phase [47]. Annealing the milled $NiFe_2O_4$ has turned it to a structural state similar to the bulk one, and its magnetic properties are gradually restored [61]. XRD show that the Ni/Fe_2O_3 mixtures are transformed in a wüstite phase after 32 h of MA [62]. After subsequently annealed at 227-627 °C the decomposition of the wüstite phase resulted in the formation of a Ni-rich intermetallic phase and a ferrite. The nanocomposite exhibit good soft magnetic properties.

The magnetic properties of $NiFe_2O_4/SnO_2$ nanocomposite produced by MA show a large variation of hysteresis loops for the different milling times. Specimens with smaller particles displayed a superparamagnetic behaviour [63].

The properties of the nanocrystalline/nanosized ferrites prepared by different mechanical routes were reviewed in ref. [64].

In last decades, many works were dedicated to obtain, by different mechanical routes, the nanocrystalline soft magnetic powders from some alloys systems based on Fe or Ni. The most studied systems are Fe-Ni and Fe-Cu. The Fe-Cu immiscible binary system is a representative system to illustrate the possibility of the MA method to form the metastable phases, mechanically alloyed Fe_xCu_{100-x} solid solutions, which are never obtained by classical metallurgy or quenching method in immiscible binary systems.

The researches concerning alloys from Fe-Cu system produced by mechanical routes cover entire Fe-Cu diagram: Fe-rich [65-74], Fe-Cu50% [67, 70, 71, 75, 76] and Cu-rich region [70, 73, 74, 77-79]. The problems involved in mechanical alloying in Fe-Cu system are reviewed in ref. [80]. It has been shown that metastable Fe-Cu phases can be formed by mechanical alloying. The mechanical alloying in the immiscible Fe-Cu system is kinetically governed by the atomic shear events and by shear-induced interdiffusion processes. By HRTEM, EDS and electron diffraction analyses it was found that an $\alpha \rightarrow \gamma$ phase transformation occurs by simultaneous shearing process when the Cu content reaches 20 at. % in bcc-$Fe_{rich}Cu$ grains with the grain size of about 20 nm. Further milling promotes the interdiffusion between fcc-$Fe_{rich}Cu$ and fcc-$FeCu_{rich}$, favored by the similarity of the lattice structures, until a complete fcc-Fe-Cu solid solution forming [75]. Generally, the solubility limit can be easily extended at 20 at% Cu in bcc phase and 6o% Fe in fcc phase [69]. A milling map of the Fe-Cu system, figure 2, show that it is possible to extend to solubility limit both for bcc and fcc phases by increasing the milling time. This improvement of the solubility is very difficult, because the excess milling leads to the precipitation of bcc Fe from fcc solid solution [67]. A comparison between different methods to extend the solubility limit in Fe-Cu system is presented in ref. [68]. It is shown that the high intensity mechanical alloying (ball milling) produces the higher extended solid solution that liquid quenching, thermal evaporation or sputtering methods [68]. The annealing of the mechanical alloyed fcc Fe-Cu solid solution induces a precipitation of the Cu and Fe atoms from solid solution. The Mössbauer spectra, in samples annealed at lower

temperatures (about 250 °C), indicates that during thermal decomposition of the fcc-$Fe_{60}Cu_{40}$ phase the Fe atoms cluster in α-Fe. By contrast, the Fe atoms in the core of nano-sized crystals first cluster in γ-Fe cohering to the fcc matrix at a higher temperature (about 350 °C) and then transform to α-Fe for further annealing [72]. From magnetization measurements it was found a thermal decomposition of the fcc-$Fe_{50}Cu_{50}$ phase, at 200 °C, into fcc-Fe, fcc-$Fe_{rich}Cu$, fcc-$Cu_{rich}Fe$ and bcc-Fe phases [80].

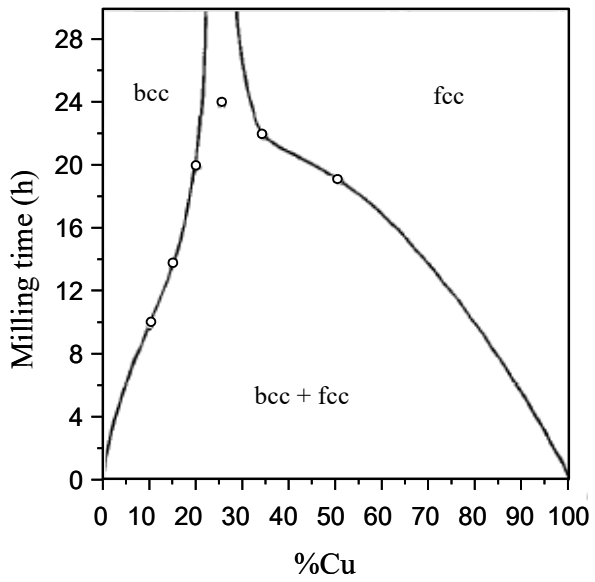

Fig. 2. Milling map of mechanically alloyed Fe-Cu system [67]. Reprinted from [67], Copyright (1997), with permission from Elsevier.

Generally, by mechanical alloying in Fe-Cu system have been produced nanocrystalline powders with the crystallite size between 3 and 50 nm, depending on milling conditions and phases composition [69, 71, 72, 75-77, 79]. It was also found that the bcc phase has considerable smaller crystallites and larger root-mean-squared (rms) strains than does the fcc phase for both lower and higher milling intensity [68].

The Fe-Cu alloys obtained by mechanical alloying present very interesting magnetic properties. Despite both Cu and Fe metals with fcc structures are nonmagnetic, the substitution of Cu atoms by Fe in fcc-Cu lattice leads to the formation of a random solid solution with the appearance of the ferromagnetic order. It was shown that the ferromagnetism (Fe-Fe positive exchange interactions) in the mechanically alloyed Fe–Cu originates when the atomic volume is expanded by a certain value (5.3% of γ-Fe, regardless of copper content), and when a certain number of neighboring iron atoms exist to percolate the ferromagnetic interaction and possibly to induce the magnetic moment on iron [70].

The mixture of Cu and bcc Fe (α-Fe) is magnetically soft with low coercivity [81,82]. The lowest coercivity was obtained in $Fe_{80}Cu_{20}$ MA powder annealed at 250 °C in order to stabilise the metastable bcc phase, figure 3. At this temperature they succeeded to minimise the residual strain and in the same time the temperature, being smaller than the recrystallisation temperature, do not favour the increasing of the nanocrystallites. Heat treatments at higher temperatures will produces recrystallisation and consequently the increasing of the crystallites will results in increasing of the anisotropy [83]. In the case of the fcc $Fe_{50}Cu_{50}$ solid solution an improvement of the coercive field, remanence induction and saturation induction, comparatively with as-milled powders has been found by isothermally annealing at 450 °C. This behaviour was explained in terms of the precipitation of nanocrystalline/ultrafine Fe in Cu matrix by a spinodal decomposition [76]. A rich synthesis on the coercivity in nanocrystalline alloy powder prepared by MA is given in the reference [83].

Magnetoresistivity measurements performed at 77 K have shown giant magnetoresistance (GMR) behaviour in samples with Fe concentration between 10 and 45 at%. The highest values of GMR ratio were reached at 20 Fe at % ($\Delta\rho/\rho$ = 1% for as-prepared samples milled for 75 hours and 2.75% for as-prepared samples milled for 20 hours [78].

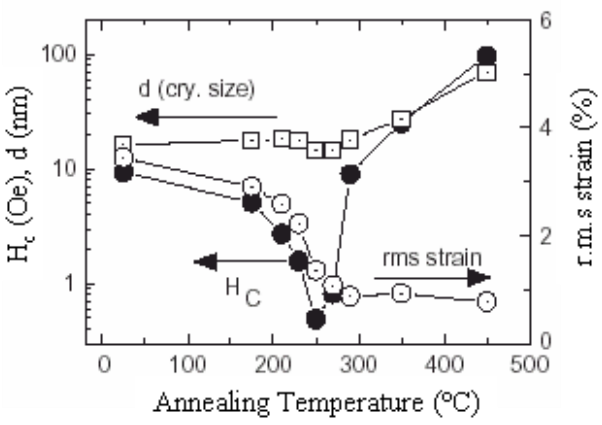

Fig. 3. Coercivity field, H_c, crystallize size, d, and r.m.s. strain as a function of annealing temperature in mechanically alloyed $Fe_{80}Cu_{20}$ powder. Reprinted from [83], Copyright (2004), with permission from Elsevier.

The Invar effect was observed in Fe-Cu solid solutions by means of lattice thermal expansion and magnetisation measurements [73]. By correlating data of the X-ray Magnetic Circular Dicroism and Extended X-ray Absorption Fine Structure it was shown that there exist two magnetic states of the iron atoms in fcc Fe-Cu alloys. Thus, the Invar effect was explained by competition between ferromagnetic-antiferromagnetic interactions, arising from the different local arrangements of the Fe atomic magnetic moments in the fcc structure [74].

The most studied alloys by mechanical routes belong to the Fe-Ni system. This interest is justified by both fundamental researches and applications. Different mechanical routes (mechanical alloying - dry or wet milling, mechanical alloying combined with annealing, two step mechanical alloying, mechanical alloying with

inserting nanocrystalline germs of the reaction product) and very different milling conditions have been used to produce nanocrystalline Fe-Ni powders [29]. The researches concerning Ni-Fe alloys produced by mechanical routes cover entire Ni-Fe diagram: Fe-rich [84-100], Fe-Ni50% [85-88, 95, 96, 99, 100-102] and Ni-rich region [85-87, 101, 103-115]. Very rich analysis of the phase transformation in $Fe_{1-x}Ni_x$ ($10 \leq x \geq 90$ at%) alloys by mechanical alloying and subsequent annealing was reported [85-87, 93]. It was shown that single phase solid solution of MA samples is significantly wider than that of thermodynamically stable alloys. A synthesis concerning the phases which could be obtained by mechanical alloying is presented by comparison with the equilibrium phase diagram in the Fe-Ni alloys, figure 4. The chemical composition of the alloys prepared by MA, the references and the phases reported are given this figure. When, at the same chemical composition, different authors report different phase's composition, this is shown by dotted line combined with number of the references. It can be seen a considerable extension of the solubility limit and also the obtaining a bct phase by MA. The nanocrystalline Ni_3Fe intermetallic compound was produced by mechanical alloying of elemental Ni and Fe powders and annealing [101, 103-116]. The Ni_3Fe intermetallic compound was obtained after 8-10 hours of milling. The mean crystallite sizes of about 22 or 12 nm were obtained after 12 and respectively 52 hours of milling and 3 hours of annealing at 330 °C [106, 107].

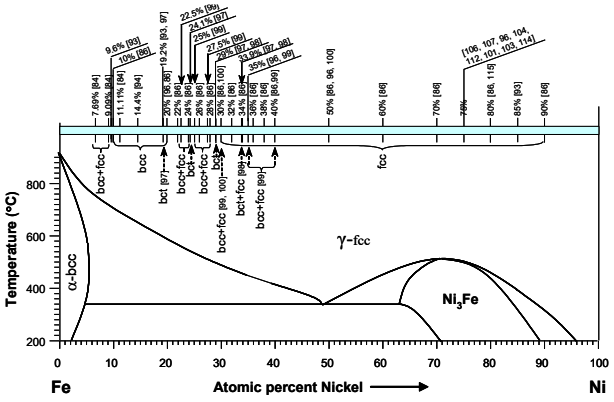

Fig. 4. A synthesis concerning the phases which could be obtained by mechanical alloying by comparison with the equilibrium phase diagram in the Fe-Ni alloys. The dotted lines (combined with number of the references) indicate other phases than usually reported.

The magnetic properties of the Ni-Fe powders obtained by MA depend on the milling conditions and of the structure. It was been proved that the milling performed in the "friction mode processes" (Ω « ω, where Ω is the rotation speed of the disk on which the vial holders are fixed and ω is the rotation speed of the vial, [117]) leads to the formation of alloys exhibiting a soft magnetic behaviour [89, 90]. A strong decrease of the coercive field versus crystallite size appears especially for crystallite size smaller than 20 nm and a limit value of the H_C = 110 A/m was obtained for Fe-Ni 20 at% after 96 hours of milling [91]. An interesting result was obtained for $Fe_{65}Ni_{35}$ alloys, which had not Invar anomaly as suggested by the equilibrium diagram [96]. A higher Curie temperature than that for the equilibrium alloys has been observed for Fe-Ni 35 at% and Fe-Ni 50 at% [96].Many authors report an increasing of the magnetisation with increasing the milling time [89, 91, 96, 104-106,107]. This behaviour is found to be linked to the grain size reduction [89-91,111]. In the case of Ni_3Fe, it was found that M_s decreases at milling time longer than 20 hours due to presence of anti-site defects in structure, induced by milling [105-107]. An annealing reduces the anti-site defects and a small increase of the magnetisation in comparison with the as milled samples is observed after annealing [105-107]. A fall in the M_s value was observed for a mean grain size of 8 nm and it was explained by the presence of SPM particles [112].

The progressive synthesis of Ni_3Fe phase by MA and subsequent annealing was checked by XRD and magnetic measurements [106, 107]. It was found that the spontaneous magnetisation tend to a saturation value by Ni_3Fe compound formation. Assuming the M_S as a control parameter of the alloying process by milling and subsequent annealing, a *Milling – Annealing – Transformation* (MAT) diagram was proposed, figure 5 [107]. In this diagram the line M_S = constant corresponds to the milling time – annealing time pairs for which the Ni_3Fe phase is formed in the whole volume of the sample and divide the diagram in to two side.

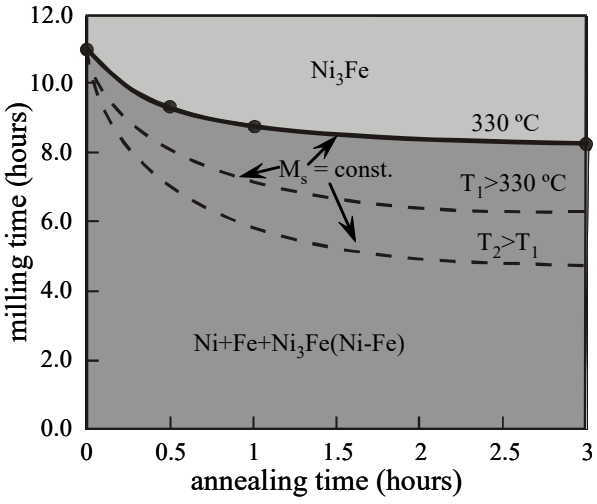

Fig. 5. The Milling – Annealing – Transformation (MAT) diagram for Ni3Fe intermetallic compound obtained by mechanical alloying and annealing. Reprinted from [107], Copyright (2003), with permission from Elsevier.

Because of their attractive soft magnetic properties the Fe-Co powders have been produced in the nanocrystalline state by MA. It was found that in the case of $Fe_{50}Co_{50}$ and $Fe_{rich}Co$ alloys the milling implies diffusion of hcp-Co into α-Fe and finally a disordered bcc-FeCo solid solution is obtained [118-120]. A coexistence of the hcp and fcc phase and an evolution of the hcp/fcc ratio with milling time have been observed for Co-10 at% Fe [121]. It was shown that the coercivity is directly affected by the crystallite size, but not by hcp/fcc phase's ratio [121]. A comparison between $Fe_{50}Co_{50}$ powders producing by MA and mechanochemical alloying (MCA), which consists in milling and hydrogen reduction of the Fe_2O_3 and Co_3O_4 powders is presented in [122]. The MCA powder exhibit a low coercivity (3.4 kA/m) and good permeability compared with MA powder, as a consequence of the formation of ordered structure and a relaxation of the internal stresses by MCA method [122]. A cyclic operation of MA (which changes the milling velocity periodically to improve the milling efficiency) by using a horizontally rotary ball mill was performed for different composition of Fe-Co alloys, covering all phase diagram [123]. By cyclic operation was obtained a small-grained structure with less milling time, comparatively with the conventional MA method. The saturation magnetisation has a maximum value at the composition of 30 at% Co for the Fe-Co powders cyclically operated for 30 h [123]. The relatively high coercive field of the as-milled powders strongly decreases by annealing, due to the removing of the internal stresses induced by milling [123].

A notable magnetic softness produced by a short time annealing (4 minutes) at low temperature (402 °C) was observed in $Fe_{50}B_{50}$ powders obtained by MA (200 h milled sample). By this magnetic softness the coercive field was decreased from thousands of A/m to tens of A/m. This behaviour was explained by improvement of the exchange coupling between α-Fe and Fe_2B crystallites and the amorphous matrix by annealing, the phase composition of the alloy remaining unchanged by low temperature annealing [124].

Many works on the ternary and polynary alloys based on Fe and Ni obtained by mechanical routes have been reported. The nanocrystalline Supermalloy powders (Ni-Fe-Mo) have been obtained from a mixture of pre-alloyed Ni_3Fe and Mo [125, 126] and from 79Ni-16Fe-5Mo (wt%) elemental powders mixture [127-131]. A minimum in the spontaneous magnetisation vs. milling time shows the presence of different processes in the Supermalloy formation by milling [76]. The coercivity was found to be dependent on the grain size and the domain wall width was estimated at 15 nm [125]. New data about obtaining Ni-Fe-Cu-Mo powders by mechanical alloying and subsequent annealing are recently published [130-133]. Finemet alloys obtained by mechanical alloying, having soft magnetic properties inferior to those of melt-spun ribbons, have been reported also [134].

It is worth to note that some Cu-based nanocrystalline alloys obtained by MA present a giant magnetoresistance effect (GMR) after annealing. The GMR effect have been observed on the $Cu_{90}Co_{10}$ [135], $Co_{20}Ni_xCu_{80-x}$ [136] and $(Co_{0.7}Fe_{0.3})_{20}Cu_{80}$ [137] nanocrystalline mechanically alloyed powders. The largest GMR effect (22 % at 10 K) has been observed on the $(Co_{0.7}Fe_{0.3})_{20}Cu_{80}$ sample annealed at 500 °C [137].

The coercivity in the nanocrystalline soft magnetic mechanically alloyed powders depends on the long-range fluctuations in the residual stresses, coupled to total anisotropy factor via the magnetostriction effect of the alloys. Starting from this assumption, the "random anisotropy model" was modified in order to take into account the residual stress in the mechanically alloyed nanocrystalline powders [138].

The nanocrystalline soft magnetic powders produced by mechanical alloying techniques are used like starting materials to design new magnetic materials by powder consolidation. The powder consolidation with preserving the nanocrystalline structure can be made by field activated pressure assisted sintering (FAPAS) and spark plasma sintering (SPS) methods [24] or by producing of the soft magnetic composites. Some applications of these nanocrystalline powders like microwave absorbing or soft composite magnetic materials have been reported [94, 139-141].

3. Hard nanocrystalline magnetic materials obtained by mechanical alloying

Mechanical alloying has been extensively applied to synthesize various metastable phases exhibiting exciting magnetic properties including hard magnetic materials. For the preparation of rare-earth permanent magnetic materials, it is necessary to carry out MA in inert atmosphere. The subsequent annealing of MA materials favours the formation of metastable phases and even of equilibrium phases at high temperatures. A review about the MA and the physical properties of the Nd-Fe-B magnets and the Sm-Fe-X phases (X = V, Ti, Zr, N, C) with ultrahigh coercivity can be found in Schultz and al. [142]. Nd-Fe-B magnets obtained by MA have magnetic properties comparable to rapid quenching materials. High energy products of 326 kJ/m^3 were reported. An excellent overview on the recent developments in nanocrystalline rare earth–transition metal magnets obtained by high energy ball milling, melt spinning and hydrogen assisted methods and hot deformation is given by Gutfleisch et al [1].

New hard magnetic phases were found in Sm-Fe-X alloys obtained by MA. Coercivity of 9.6-12 kA/m X=V, $ThMn_{12}$ crystal structure, 51.6 kA/m X=Ti, A_2 phase (Nd_5Fe_{17} structure) [142] or 24 kA/m X=N or C [142, 143] were obtained. The physical properties of as cast, annealed

and mechanical milled Sm-Co-Cu-Ti magnets are compared in Table 2 [144]. All samples exhibit uniaxial anisotropy with Curie temperature higher than 650 °C. A range of exchange-coupled two-phase nanocomposite hard magnetic $Sm_2Fe_{17}N_3$ and soft α-Fe were prepared by MA and subsequent annealing and nitrogenation to optimize the hysteresis loop shape [145]. The main variables were the crystallisation conditions, the nitrating treatment and the chemical additives. A model of nitrogen diffusion in the two-phase nanocomposite was proposed. The Fe presence improves the nitrogenation of Sm_2Fe_{17} phase. TEM and SEM studies evidenced that adding 2 at% of Zr or Ta reduce the grain size from 20-30nm to 10-20 nm and improves the hysteresis curve. The complete reversibility of returning to remanence was observed in demagnetisation curve. Mössbauer studies revealed that the boundary phase between crystallites constitutes 15 vol% of the nanocomposite. MA of elemental powders in the composition range Sm_xFe_{100-x} was successfully used to synthesize a $SmFe_7$ phase and, for higher milling time, Sm_2Fe_{17} [146]. After nitrogenation, T_c raises to 480 °C. The best results are obtained in nitrogenated samples with x = 12.5: ${}_iH_c$ = 3.42 MA/m, B_r = 0.8 T and $(BH)_{max}$ = 114.4 kJ/m^3. Nitrogenation of MA Sm-Fe alloys improves the magnetic properties of $Sm_2Fe_{17}C_x$/α-Fe nanocomposites [145, 146].

Nanocomposite Sm_2Fe_{17}-Cu alloys have been fabricated using low energy co-milling of mechanical alloyed Sm_2Fe_{17} and Cu powders [147]. Nanocomposite magnetic properties have been controlled by milling conditions. There were produced nanocomposite Sm_2Fe_{17}-Cu with suitable magnetic properties and microstructure for high-density recording.

Structural and magnetic measurements of mechanically milled $SmCo_5$ suggest that milling produces small $SmCo_5$ crystallites separated by a glassy Sm-Co interphase [148]. The volume fraction of the interphase increases by additional milling. An important increase of coercivity accompanied by remanence ratio on the order of 0.7 is induced by milling.

The structure, phase transformation and magnetic properties of $Sm_yFe_{100-1.5y}C_{0.5y}$ (y = 10 – 20) alloys prepared by MA have been studied by Geng et al. [149]. The $Sm_2Fe_{17}C_x$ structure is present for high y values while $Sm_2Fe_{14}C$ appears for smaller y values. $Sm_2Fe_{17}C_x$ and $Sm_2Fe_{14}C$ coexist under certain conditions. Re-milling and annealing had been developed to obtain good magnetic properties; ${}_iH_c$ = 640 MA/m and $(BH)_{max}$ = 84.8 kJ/m^3 in $Sm_{14}Fe_{79}C_9$ and $Sm_{20}Fe_{70}C_{10}$. High energy ball milling of Fe-Sm powders and subsequent annealing leads to the disordered $SmFe_9$ phase with $TbCu_7$-type hexagonal P6/mmm structure, which appears as the precursor of the ordered R $\overline{3}$ m Sm_2Fe_{17} phase [150]. The effect of Si on nanocrystalline $SmFe_9$ phase with $TbCu_7$-type hexagonal P6/mmm structure was studied by HREM, XRD, Mössbauer spectrometry and magnetic measurements [151]. Si occupies the 3g site and T_c is raised by around 30 K compared to the equilibrium $Sm_2(FeSi)_{17}$ alloys. The optimal values of M_r/M_s=0.81 and $(BH)_{max}$=54.8 kJ/m^3, have been achieved for nanocomposite $SmFe_7C_x$/α-Fe obtained by MA [152]. The maximum specific energy of MM $PrCo_5$ powder has been enhanced by introducing the soft Pr_2Co_{17} phase [153].

Mechanical alloying of Co and W with $Nd_2Fe_{14}B$ influences the structure and magnetic properties of nanocomposite $Nd_2Fe_{14}B$/α-Fe magnets [154]. W addition leads to the decreasing of the grain size and remanence while Co addition increases the exchange length and decreases the crystallisation temperature, the remanence and $(BH)_{max}$. The influence of Fe, Ti, V, Cr, Mn, Co and Al on the phase constitution and magnetic properties of Nd-Fe-B alloys was studied in MA samples by Liu et al. [155].

Mechanical alloying of Co and W with $Nd_2Fe_{14}B$ influences the structure and magnetic properties of nanocomposite $Nd_2Fe_{14}B$/α-Fe magnets [154]. W addition leads to the decreasing of the grain size and remanence while Co addition increases the exchange length and decreases the crystallisation temperature, the remanence and $(BH)_{max}$. The influence of Fe, Ti, V, Cr, Mn, Co and Al on the phase constitution and magnetic properties of Nd-Fe-B alloys was studied in MA samples by Liu et al. [155].

Table 2. Structural and room-temperature coercivity of Sm-Co-Cu-Ti intermetallic compounds [144].

Type	Compound	Structure type	$\mu_0 H_c$(T)
As-cast	$SmCo_7$	$TbCu_7 + Th_2Zn_{17}$	0.05
	$SmCo_{6.7}Ti_{0.3}$	$TbCu_7$	0.12
	$SmCo_{6.7}Cu_{0.3}$	$TbCu_7$	0.10
	$SmCo_{6.7}Ti0_{.3}Cu_{0.3}$	$TbCu_7$	0.15
As-cast + annealed	$SmCo_7$	$CaCu_5 + Th_2Zn_{17}$	0.12
	$SmCo_{6.7}Ti_{0.3}$	$CaCu_5 + Th_2Zn_{17}$	0.23
	$SmCo_{6.7}Cu_{0.3}$	$CaCu_5 + Th_2Zn_{17}$	0.20
	$SmCo_{6.7}Ti0_{.3}Cu_{0.3}$	$CaCu_5 + Th_2Zn_{17}$	0.26
MM + annealed	$SmCo_7$	$TbCu_7 + Th_2Zn_{17}$	0.26
	$SmCo_{6.7}Ti_{0.3}$	$TbCu_7 + Th_2Zn_{17}$	1.90
	$SmCo_{6.7}Cu_{0.3}$	$TbCu_7 + Th_2Zn_{17}$	0.70
	$SmCo_{6.7}Ti0_{.3}Cu_{0.3}$	$TbCu_7 + Th_2Zn_{17}$	2.50

Grossinger and Sato [156] reveal that nanocrystalline hard magnetic materials exhibit, due to the fact that the grain sizes are comparable to the magnetic exchange length, a specific magnetic behaviour; the increasing of the remanence is accompanied by a lower anisotropy and consequently a decreasing of the coercivity. Due to the exchange coupling between crystallites also the domain structure in nanocrystalline hard magnetic materials is

different compared with microcrystalline material. It was found that the correlation lengths of the magnetic contrast in the magnetic force microscopy, MFM, images are within the range 100– 550 nm for the Nd-Fe-B alloy, substantially larger than the median crystallite size which is 20–35 nm [157]. Nevertheless, within these correlation lengths, small fluctuations in magnetic contrast were observed on a scale down to about 20 nm, the nanocrystallite dimensions, which could explains the diminution of the coercivity.

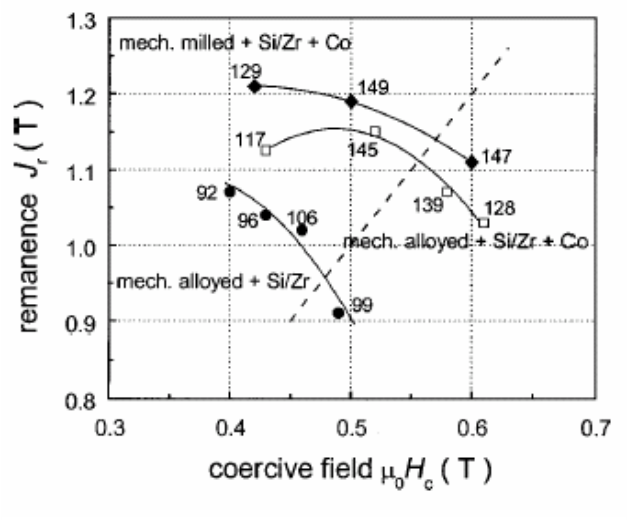

Fig. 3. Remanent polarization J_r as a function of coercive field $\mu_0 H_c$ for three types of NdFeB powders.The numbers beside the data points quote the energy density in kJ/m³. With permission from V. Neu and L. Schultz, [159]. Copyright 2001, American Institute of Physics.

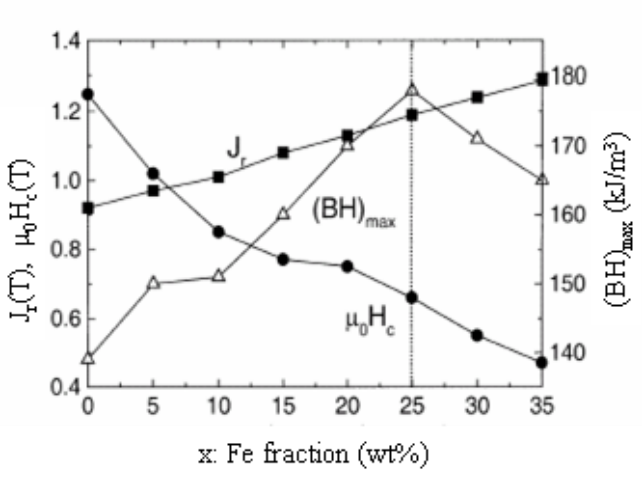

***Fig. 4**. Evolution of remanence, J_r ; coercivity, $\mu_0 H_c$ and energy product, $(BH)_{max}$ vs. Fe-fraction in $Pr_9Nd_3Dy_1Fe_{72}Co_8B_{6.9}Zr_{0.1}$+x wt% Fe nanocomposite. Dotted line indicates the Fe-fraction which leads to the best combination of magnetic properties. Reprinted from [160], Copyright (2003), with permission from IEEE.*

The substitution, mainly of Fe, by Co, Si or Zr in Nd-Fe-B/Fe based nanocomposite could improve the magnetic properties of two-phase nanocomposite materials prepared by milling and annealing [159]. This behaviour is mainly explains by the refinement of the microstructure by Si or Zr and the increasing of the Curie temperature and the saturation magnetisation by Co. The results of different approaches are given in figure 3 [159]. The sample prepared by mechanical milling and annealing present better properties in comparison with those obtained by mechanical alloying and milling. Thus, mechanically milled and optimally annealed NdFeB powders show high energy densities of $(BH)_{max}$ =149 kJ/m³ for a favourable phase ratio of 70 vol% hard and 30 vol% soft magnetic phase. An analysis of recoil loops measured during the demagnetization process has been carried out to obtain information about the nature of intergrain interactions in nanocrystalline isotropic $Pr_9Nd_3Dy_1Fe_{72}Co_8B_{6.9}Zr_{0.1}$+x wt% Fe (x=5-35) magnets [160]. Figure 4 shows the magnetic properties vs. Fe content for the complete series obtained by mechanical milling and annealing. The maximum value for the $(BH)_{max}$=178kJ/m³ is achieved for an iron content of 25 wt.%. For Fe content lower than 25 wt.% the coercive field is higher than one-half of J_r, i.e., $(BH)_{max}$ is mainly controlled by remanence resulting in an increase of $(BH)_{max}$ with increasing J_r. At higher Fe contents the coercive field is smaller than one-half of J_r and $(BH)_{max}$ decreases as a consequence of irreversible demagnetization processes[160]. Due to the temperature dependence of the exchange length, the exchange interactions between nanograins are temperature dependent. Consequently, as for the soft magnetic materials, the exchange coupling between crystallites has an evolution vs. temperature [156, 160].

The influence of the milling and annealing conditions on the structural and magnetic behaviour of mechanically-milled $SmCo_5$/α-Fe alloys has been studied [161].

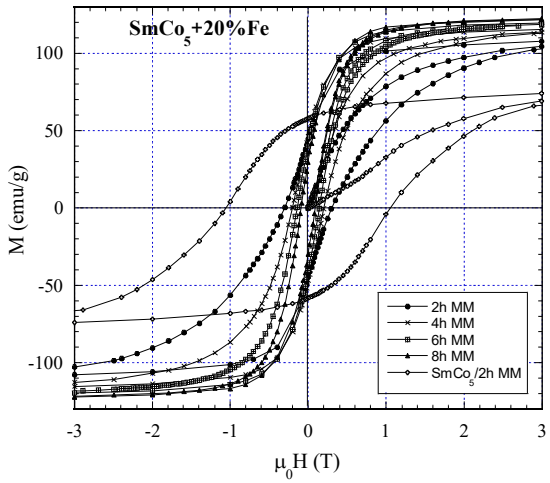

Fig. 5. Room temperature hysteresis curves recorded for the $SmCo_5$ +20% Fe composite samples milled from 2 to 8 hours compared to that of the hard phase $SmCo_5$ milled for 2 hours.

The structural and microstructural evolution of the samples was followed by X-ray diffraction and electronic microscopy. The annealing of MM samples induces a refinement of the structure. Nanosize crystallites are obtained for the long milling time. The grain size, according to Scherrer's formula, is derived to be of about 18 nm. The coercive field, the remanent magnetisation and the degree of the exchange coupling between the hard magnetic grains and the soft α-Fe grains were studied from magnetic measurements and Mössbauer spectrometry [162]. After annealing, the demagnetisation curve exhibits a smooth shape testifying for a good coupling between the hard $SmCo_5$ and soft α-Fe magnetic phases, Fig. 5 and 6 [162].

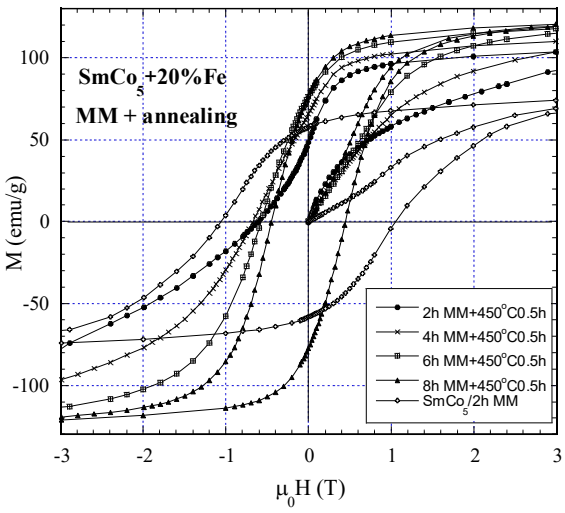

Fig. 6. Room temperature hysteresis curves for the $SmCo_5$ +20% Fe samples milled for 2 to 8 hours and annealed at 450 °C for 0.5 hours. The hysteresis curve of the hard phase $SmCo_5$ milled for 2 hours is given for comparison.

The increase of the annealing temperature or the annealing time improves the rectangularity of the hysteresis curve and leads to an improvement of both coercivity and remanence. According to Mössbauer spectrometry investigation, the mean hyperfine field of the soft α-Fe contribution increases with the milling time. This behaviour could be connected with an increase of the Co content in the α-Fe phase. Also, a contribution attributed to Fe atoms that diffused into the $SmCo_5$ phase during milling is evidenced in the Mössbauer spectra of both as-milled and annealed samples [162]. The increase of the Fe content from 20 to 30 wt% in $SmCo_5$/α-Fe nanocomposite gives a pourer exchange coupling between $SmCo_5$ hard phase and α-Fe soft magnetic phase [163]. $SmCo_3Cu_2$/α-Fe nanocomposites have been obtained by mechanical milling of a $SmCo_3Cu_2$+30 wt% α-Fe mixture and subsequent annealing [164]. A dramatic decrease in both the coercivity and the remanence was observed after milling. The annealing does not succeed to improve significantly this behaviour, Fig. 7. This behaviour can be attributed either to the Fe enrichment of the hard phase and/or to the deterioration of the characteristic microstructure [165] during milling. Indeed a two phases microstructure made of Cu rich and Co rich $Sm(CoCu)_5$ phases has been reported to favour the high performance of $Sm(CoCu)_5$ type magnets. Unlike what was found with the $SmCo_5$/Fe system where good coupling and coercivity were obtained [162], the low intrinsic anisotropy of the $SmCo_3Cu_2$ phase [165] may prevent significant coercivity to be obtained in the $SmCo_3Cu_2$/Fe system.

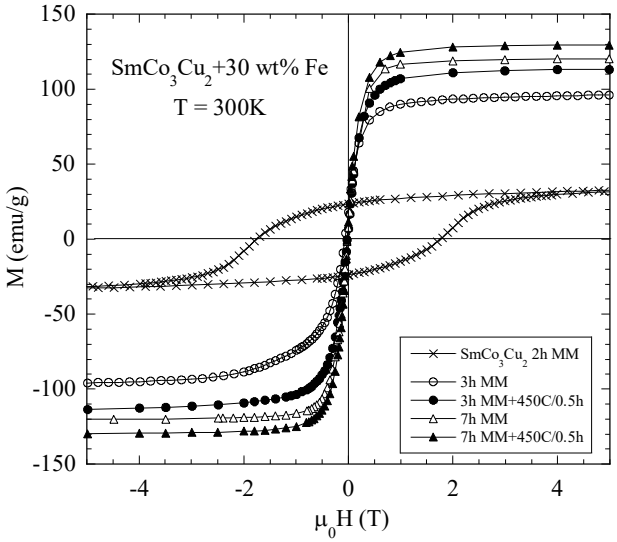

Fig. 7. Room temperature hysteresis cycles recorded for the $SmCo_3Cu_2$+30wt% Fe composite samples milled 3 and 7 h and annealed at 450 °C for 0.5 h. The hysteresis curve of the $SmCo_3Cu_2$ hard phase 2 h MM is given for comparison.

Mechanical milling has been applied in order to obtain $(Nd_{0.92}Dy_{0.08})_2Fe_{14}B$/α-Fe magnetic nanocomposite [166]. The coercivity and the remanence are very sensitive to the synthesis process and can be improved by adjusting the milling and/or annealing conditions, figure 8. This behaviour was connected to the strength of the exchange coupling between the hard and the soft magnetic nanocrystallites. The optimum magnetic behaviour was obtained for a heat treatment at temperatures between 550 °C and 600 °C for 1.5 hours. The coercivity and the remanence decrease for the nanocomposite samples annealed at temperatures higher than 650 °C. This evolution shows that at these temperatures some recrystallisation starts and also chemical reaction between the two phases may occur, whereas the exchange coupling becomes poorer.

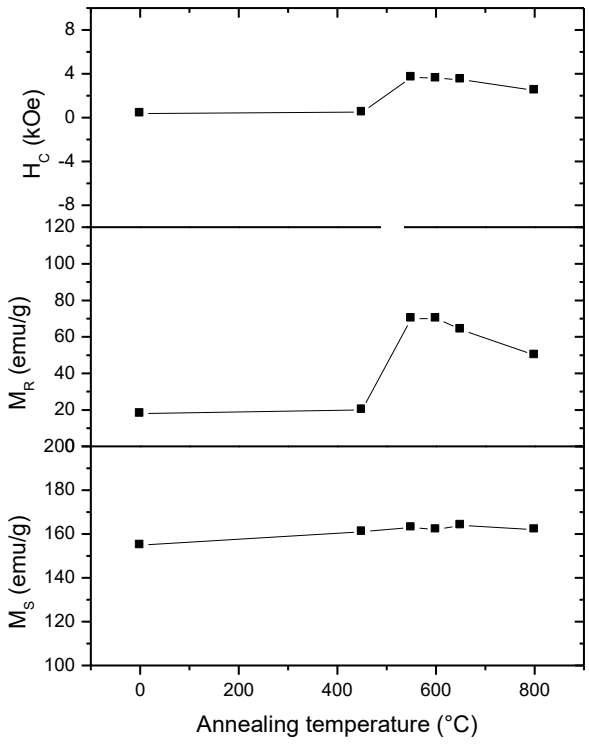

Fig. 8. The evolution of the saturation magnetization (at 10T), the remanent magnetisation and the coercivity of the 6 hours mechanically milled $(Nd_{0.92}Dy_{0.08})_2Fe_{14}B/\alpha$-Fe powder samples vs. the annealing temperature.

4. Conclusions

Besides to the interest in fundamental study, the nanocrystalline and nanocomposite soft or hard magnetic materials present very promising magnetic properties for applications; a strength remanence and high energy product, for nanocomposite spring magnets, and low coercivity, high permeability and improved resistivity for soft nanocrystalline materials. Consequently these materials are widely studied for a better understanding of the fundamental properties and also for the applications. The isotropic magnets produced from nanocomposite magnetic materials present a specific energy up to 160-178 kJ/m^3 [160] greater than the best isotropic non-interacting NdFeB based magnets, 96-112 kJ/m^3 with a theoretical maximum energy of 126 kJ/m^3 [167,168]. In last decade many research concerning nanocrystalline magnetic materials produced by mechanical routes has been reported. The nanocrystalline powders, obtained by MA or MM techniques, represent a reliable alternative to produce nanomaterials.

Acknowledgement

This work has been supported by the CEEX and CNCSIS grants. The authors are grateful to the Romanian Ministry of Education and Research for financial support.

References

[1] Gutfleisch, A. Bollero, A. Handstein, D. Hinz, A. Kirchner, A. Yan, K.H. Muller, L. Schultz, J. Magn. Magn. Mater. **242-245**, 1277 (2002).
[2] R. Hasegawa, J. Magn. Magn. Mater. **304**, 187 (2006).
[3] G. C. Hadjipanayis, J. Magn. Magn. Mater. **200**, 373 (1999).
[4] Y. Yoshizawa, S. Oguma, K. Yamauchi, J. Appl.Phys. **64,** (1988) 6044.
[5] G. Herzer, M. Vazquez, M. Knobel, A. Zhukov, R. Reininger, H.A. Davies, R. Grossinger, J. L. Sanchez, J. Magn. Magn. Mater. **294**, 152 (2005).
[6] K. H. J. Buschow, Handbook of Mag. Mater., Ed. K.H.J. Buschow **10,** 463 (1997).
[7] R. Coehoorn, D. B. de Mooij, C. De Waard, J. Magn. Magn. Mater. **80**, 101 (1989).
[8] R. Skomski, J. Phys.: Condens. Matter. **15**, R841 (2003).
[9] R. Skomski, J. M. D. Coey, Permanent Magnetism, Institute of Physics Publishing, Bristol 1999.
[10] E. F. Kneller, R. Hawig, IEEE Trans. Mag. **27**, 3588 (1991).
[11] Z. D. Zhang, W. Liu, J. P. Liu, D. J. Sellmyer, J. Phys. D: Appl. Phys. **33**, R217 (2000).
[12] K. Hono, D. H. Ping, Y. Q. Wu, Proceedings 22nd Ris∅ Int. Symp. On Material Science, 2001 Roskilde, Denmark.
[13] J. Petzold, J. Magn. Magn. Mater. **242-245**, 84 (2002).
[14] E. E. Fullerton, J. S. Jiang, S. D. Bader, J. Magn. Magn. Mater. **200**, 392 (1999).
[15] C. Kittel, Rev. Mod. Phys. **21**, 541 (1949).
[16] G. Herzer, IEEE Trans. Magn. MAG-25 (1989) 3327; IEEE Trans. Magn. **MAG-26**, 1397 (1990).
[17] R. Hasegawa, J. Magn. Magn. Mater. **215–216**, 240 (2000).
[18] T. Kulik, J. Non Crystalline Solids **287**, 145 (2001).
[19] G. Herzer, J. Magn. Magn. Mater. **294**, 99 (2005).
[20] G. Herzer, Handbook of Mag. Mater., Ed. K.H.J. Buschow, **Vol 10**, 415 (1997).
[21] C. C. Koch, J. D. Whittenberger, Intermetallics **4**, 339 (1996).

[22] C. Suryanarayana, Progr. Mater. Sc. **46**, 1 (2001).
[23] P.H. Shingu, K.N. Ishihara, Mater. Trans. JIM **36**, 96 (1995).
[24] E. Gaffet, G. Le Caër, Mechanical Processing for Nanomaterials, in Encyclopaedia of Nanoscience and Nanotechnology, vol.X, Ed. by H.S. Nalwa, American Sci. Publishers (2004).
[25] A. R. Yavari, Mater. Trans. JIM **36**, 228 (1995).
[26] D.L. Zhang, Progr. Mater. Sci. **49**, 537 (2004).
[27] L. Shultz, Philos. Mag. B61 (1990) 453; L. Shultz, J. Wecker, Mater. Sci. Eng. **89**, 127 (1988).
[28] B. S. Murty, S. Ranganathan, Int. Mater. Reviews, **43**, 101 (1998).
[29] I. Chicinaş, J. Optoelectron. Adv. Mater. **8,** 439 (2006).
[30] G. F. Goya, H.R. Rechenberg, J. Phys.: Condens. Mater. **10**, 11829 (1998).
[31] S. F. Mustafa, M.B. Morsi, Mater. Lett. **34**, 241 (1998).
[32] V. Šepelák, M. Menzel, I. Bergmann, M. Wiebcke, F. Krumeich, K.D. Becker, J. Magn. Magn. Mater. **272-276**, 1616 (2004).
[33] M. Menzel, V. Šepelák, K.D. Becker, Solid State Ionics **141-142**, 663 (2001).
[34] J.P. Muňoz Mendoza, O. E Ayala Valenzuela, V. Corral Flores, J. Matutes Aquino, S. D. De la Torre, J. Alloys Comp. **369**, 144 (2994).
[35] G. F. Goya, H.R. Rechenberg, J. Magn. Magn. Mater. **203**, 141 (1999).
[36] F. Padella, C. Alvani, A. La Barbera, G. Ennas, R. Liberatore, F. Varsano, Mater. Chem. Phys. **90**, 172 (2005).
[37] J. Ding, P.G. McCormick, R. Street, Solid State Commun. **95**, 31 (1995).
[38] G. F. Goya, H. R. Rechenberg, J. Z. Jiang, J. Appl. Phys. **84**, 1101 (1998).
[39] J. Z. Jiang, G. F. Goya, H. R. Rechenberg, J. Phys.: Condens. Mater. **11**, 4063 (1999).
[40] V. Šepelák, D. Baabe, D. Mienert, D. Schultze et al., J. Magn. Magn. Mater. **257**, 377 (2003).
[41] V. Šepelák, D. Baabe, K.D. Becker, J. Mater. Synth. Proces. **8**, 333 (2000)
[42] C. N. Chinnasamy, A. Narayanasamy, N. Ponpandian et al., Scripta Mater. **44**, 1407 (2001).
[43] C.N. Chinnasamy, A. Narayanasamy, N. Ponpandian, K. Chattopadhyay, Mater. Sci. Eng. **A304-306**, 983 (2001).
[44] S.D. Shenoy, P. A. Joy, M.R. Anantharaman, J. Magn. Magn. Mater. **269**, 217 (2003).
[45] V. Šepelák, M. Menzel, K. D. Becker, F. Krumeich, J. Phys. Chem. **B106**, 6672 (2002).
[46] V. Šepelák, D. Baabe, D. Mienert. F. J. Litterst, K. D. Becker, Scripta`Mater. **48**, 961 (2003).
[47] M.E. Rabanal, A. Várez, B. Levenfeld, J.M. Torralba, J. Mater. Process. Techn. **143-144**, 470 (2003).
[48] C.N. Chinnasamy, A. Narayanasamy, N. Ponpandian et al., J. Appl. Phys. **90**, 527 (2001).
[49] C.N. Chinnasamy, A. Narayanasamy, N. Ponpandian et al., Scripta Mater. **44**, 1411 (2001).
[50] G. F. Goya, J. Mater. Sci. **39**, 5045 (2004).
[51] G. F. Goya, Solid State Commun. **130**, 783 (2004).
[52] M. E. Rabanal, A. Várez, B. Levenfeld, J.M. Torralba, Mater. Sci. Forum **426-432**, 4349 (2003).
[53] Y. Shi, J. Ding, X. Liu, J. Wang, J. Magn. Magn. Mater. **205**, 249 (1999).
[54] G. F. Goya, H.R. Rechenberg, Mater. Sci. Forum, **403** and J. Metastable and Nanocrystalline Mater. **14**, 127 (2002).
[55] S. Ozcan, B. Kaynar, M.M. Can, T. Firat, Mater. Sci. Eng. B, preprint (2005).
[56] J. Ding, P.G. McCormick, R. Street, J. Magn. Magn. Mater. **171**, 309 (1997).
[57] V. Šepelák, D. Schultze, F. Krumeich, U. Steinike, K.D. Becker, Solid State Ionics **141-142**, 677 (2001).
[58] Y. Shi, J. Ding, H. Yin, J. Alloys Comp. **308**, 290 (2000).
[59] M. Mozaffary, J. Amighian, J. Magn. Magn. Mater. **260**, 244 (1997).
[60] S. Dasgupta, J. Das, J. Eckerth, I. Manna, J. Magn. Magn. Mater., **306**, 9 (2006)
[61] V. Sepelak, D. Baabe, D. Mienert, D. Schultze, F. Krumeich, F. J. Litterst, K. D. Becker, J. Magn. Magn. Mater. **257**, 377 (2003).
[62] Y. Shi, J. Ding, S. L. H. Tan, Z. Hu, J. Magn. Magn. Mater. **256**, 13 (2003).
[63] A. S. Albuquerque, J. D. Ardisson, W. A. A. Macedo et al., J. Magn. Magn. Mater. **272-276**, 2211 (2004).
[64] V. Šepelák, I. Bergmann, S. Kips, K.D. Becker, Z. Anorg. Allg. Chem. **631**, 993 (2005).
[65] Y.Z. Yang, Y.L. Zhu, Q.S. Li, X.M. Ma, Y.D. Dong, G.M. Wang, S.Q. Wei, F.X. Liu, Y.Z. Chuang, Physica B **233**, 119 (1997).
[66] S. Wei, H. Oyanagi, C. Wen, Y. Yang, W. Liu, J. Phys.: Condens. Mater. **9**, 11077 (1997).
[67] B. Majumdar, M. Manivel Raja, A. Narayanasamy, K. Chattopadhyay, J. Alloys Comp. **248**, 192 (1997).
[68] L. B. Hong, B. Fultz, Acta Mater. **46**, 2937 (1998).
[69] P. J. Schilling, J. H. He, R. C. Tittsworth, E. Ma, Acta Mater. **47**, 2525 (1999).

[70] H. Ino, K. Hayashi, T. Otsuka, D. Isobe, K. Tokumitsu, K. Oda, Mater. Sci. Eng. **A304-306**, 972 (2001).
[71] N. Wanderka, U. Czubayko, V. Naundorf, V.A. Ivchenko, A. Ye. Yermakov, M.A. Uimin, H. Wollenberger, Ultramicroscopy **89**, 189 (2001)
[72] Y.Z. Yang, Y.L. Zhu, Q.S. Li, X.M. Ma, Y.D. Dong, G.M. Wang, S.Q. Wei, Physica B **293**, 249 (2001)
[73] P. Gorria, D. Martinez-Blanco, J.A. Blanco, Phys. Rev. B **69**, 214421 (2004).
[74] A. Orecchini, F. Sacchetti, C. Petrillo, P. Postorino, A. Congeduti, Ch. Giorgetti, F. Baudelet, G. Mazzone, J. Alloys Comp. **424**, 27 (2006).
[75] J. Y. Huang, J.Z. Jiang, H. Yasuda, H. Mori, Phys. Rev. B **58**, R11817 (1998).
[76] B. N. Mondal, A. Basumallick, P.P. Chattopadhyay, J. Magn. Magn. Mater. **309**, 290 (2007).
[77] R. A. Dunlap, D.A. Eelman, G.R. Mackay, J. Mater. Sci. Lett. **17**, 437 (1998).
[78] L. M. Socolovsky, F.H. Sánchez, P.H. Shingu, Hyperfine Inter. **133**, 47 (2001).
[79] F. Jurányi, J.-B. Suck, S. Janssen, Appl. Phys. **A74** (Suppl.), S972 (2002).
[80] J. Z. Jiang, C. Gente, R. Bormann, Mater. Sci. Eng. **A242**, 268 (1998).
[81] A. R. Yavary, P. J. Desre, T. Benameur, Phys. Rev. Lett. **68**, 2235 (1992).
[82] T. Ambrose, A. Gavrin, C. L. Chien, J. Magn. Magn. Mater. **124**, 15 (1993).
[83] R. B. Schwarz, T. D. Shen, U. Harms, T. Lollo, J. Magn. Magn. Mater. **283**, 223 (2004).
[84] Y. Liu, J. Zhang, L. Yu, G. Jia, C. Jing, S. Cao, J. Magn. Magn. Mater. **285**, 138 (2005).
[85] Yu. V. Baldokhin, V. V. Tcherdyntsev, S. D. Kaloshin, G. A. Kochetov, Yu. A. Pustov, J. Magn. Magn. Mater. **203**, 313 (1999).
[86] S. D. Kaloshin, V. V. Tcherdyntsev, I. A. Tomilin, Yu. V. Baldokhin, E. V. Shelekhov, Physica B **299**, 236 (2001).
[87] S. D. Kaloshin, V. V. Tcherdyntsev, Yu. V. Baldokhin, I. A. Tomilin, E. V. Shelekhov, J. Non-Cryst. Solids **287**, 329 (2001).
[88] E. Jartych, J. Magn. Magn. Mater. **265**, 176 (2003).
[89] R. Hamzaoui, O. Elkedim, E. Gaffet, Mater. Sci. Eng.. **A 381**, 363 (2004).
[90] R. Hamzaoui, O. Elkedim, E. Gaffet, J. Mater. Sci. **39**, 5139 (2004).
[91] R. Hamzaoui, O. Elkedim, N. Fenineche, E. Gaffet, J. Craven, Mater. Sci. Eng. **A 360**, 299 (2003).
[92] R. Hamzaoui, S. Guessasma, O. Elkedim, E. Gaffet, Mater. Sci. Eng. **Bxxx** (2005) in press
[93] V. V. Tcherdyntsev, S. D. Kaloshkin, I. A. Tomilin, E. V. Shelekhov, Yu. V. Baldokhin, Nanostr. Mater. **12**, 139 (1999).
[94] P. H. Zhou, L.J. Deng, J. L. Xie, D. F. Liang, L. Chen, X. Q. Zhao, J. Magn. Magn. Mater. **292**, 325 (2005).
[95] M. Pękała, D. Oleszak, E. Jartych, J. K. Żurawicz, Nanostr. Mater. **11**, 789 (1999).
[96] E. Jartych, J.K. Żurawicz, D. Oleszak, M. Pękała, J. Magn. Magn. Mater. **208**, 221 (2000).
[97] L.-H. Zhu, Q.-W. Huang, H.-F. Zhao, Scripta Mater. **51**, 527 (2004).
[98] L.-H. Zhu, X.-M. Ma, L. Zhao, J. Mater. Sci., **36**, 5571 (2001).
[99] J. F. Valderruten, G. A. Pèrez Alcazar, J.M. Greneche, Physica B **384**, 316 (2006)
[100] G. González, D. Ibarra, J. Ochoa, R. Villalba, A. Sagarzazu, J. Alloys Comp. (2006) doi: 10.1016/j.jalcom.2006.08.293
[101] L. H. Bennett, L. Takacs, L. J. Swartzendruber, J. Weismuller, L.A. Bendersky, a.J. Shapira, Scripta Metall. Mater. **33**, 1717 (1995).
[102] A. Djekoun, B. Bouzabata, A. Otmany, J. M. Greneche, Catalysis Today **89**, 319 (2004).
[103] I. Chicinas, C. Nitray, N. Jumate, Proc. of the 2nd Int. Conf. Powder Metall. RoPM2000, UT Press, Cluj-Napoca **2**, 637 (2000).
[104] I. Chicinas, V. Pop, O. Isnard, J.M. Le Breton, Proc. "Materiaux 2002" Congress, ISBN 2-914279-08-6, Tours, (on CD).
[105] I. Chicinas, V. Pop, O. Isnard, J. Magn. Magn. Mater. **242-245**, 885 (2002).
[106] I. Chicinas, V. Pop, O.Isnard, J.M. Le Breton, J. Juraszek, J. Alloys Comp. **352**, 34 (2003).
[107] V. Pop, O. Isnard, I. Chicinas, J. Alloys Comp. **361**, 144 (2003).
[108] Z. Spârchez, I. Chicinas, O. Isnard, V. Pop, F. Popa, J. Alloys Comp. (2006)
[109] I. Chicinaş, O. Isnard, V. Pop, J. M. Le Breton, O. Geoffroy, in New Trends in Advanced Materials, Ed. by N.M. Avram, V. Pop, R. Tetean, Editura Universităţii de Vest, Timişoara, 2005, ISBN 973-7608-41-0, 29-38
[110] Z. Sparchez, I. Chicinaş, O. Isnard, V. Pop, F. Popa, Proc. Materiaux 2006 Congrès, Dijon, France, 13-17 Nov. 2006, Proc. on CD
[111] H. N. Frase, R.D. Shull, L.-B. Hong, T.A. Stephens, Z.-Q. Gao, B. Fultz, Nanostr. Mater. **11**, 987 (1999).
[112] C. N. Chinnasamy, A. Narayanasamy, N. Ponpandian, K. Chattopadhyay, M. Saravanakumar, Mater. Sci. Eng. **A304-306**, 408 (2001).
[113] C. N. Chinnasamy, A. Narayanasamy, K. Chattopadhyay, N. Ponpandian, Nanostr. Mater., **12**, 951 (1999).
[114] B. H. Meeves, G.S. Collins, Hyperfine Interact. **92**, 955 (1994).

[115] P. Kollár, D. Olekšáková, J. Kováč, S. Roth, K. Polański, J. Magn. Magn. Magn. Mater. (2006), doi: 10.1016/j.jmmm.2006.11.044.
[116] F. Popa, I. Chicinas, O. Isnard, V. Pop, J. Optoelectron Adv. Mater. submitted
[117] M. Abdellaoui, E. Gaffet, Acta. Metall. Mater. **44**, 1087 (1995).
[118] M. Sorescu, A. Grabias, Intermetallics **10**, 317 (2002).
[119] Y. Liu, J. Zhang, L. Yu, G. Jia, C. Jing, S. Cao, J. Alloys Comp. **377**, 202 (2004).
[120] H. Moumeni, S. Alleg, J.M. Greneche, J. Alloys Comp. **386**, 12 (2005).
[121] N.E. Fenineche, R. Hamzaoui, O. El Kedim, Mater. Lett. **57**, 4165 (2003).
[122] B.-H. Lee, B.S. Ahn, D.-G. Kim, S.-T. Oh, H. Jeon, J. Ahn, Y.D. Kim, Mater. Lett. **57**, 1103 (2003).
[123] Y.D. Kim, J.Y. Chung, J. Kim, H. Jeon, Mater. Sci. Eng. **A291**, 17 (2000).
[124] J. M. Gonzáles, G.A. Pérez Alcázar, L.E. Zamora, J. A. Tabares, A. Bohórquez, J.R. Gancedo, J. Magn. Magn. Mater. **261**, 337 (2003).
[125] Y. Shen, H.H. Hng, J.T. Oh, J. Alloys Comp. **379**, 266 (2003).
[126] Y. Shen, H.H. Hng, J.T. Oh, Mater. Lett. **58**, 2824 (2004).
[127] I. Chicinas, V. Pop, O. Isnard, J. Mater. Sci. **39**, 5305 (2004).
[128] O. Isnard, V. Pop, I. Chicinas, J. Magn. Magn. Mater. **290-291**, 1535 (2005).
[129] F. Popa, I. Chicinas, O. Isnard, V. Pop, J. Optoelectron Adv. Mater., submitted.
[130] O. Isnard, I. Chicinas, F. Popa, V. Pop, Proc. "Materiaux 2006" Congrès, ISBN 978-2-9528-1400-3, Dijon, (on CD).
[131] F. Popa, O. Isnard, I. Chicinas, V. Pop, Proc. "Materiaux 2006" Congrès, ISBN 978-2-9528-1400-3, Dijon, (on CD)
[132] F. Popa, O. Isnard, I. Chicinas, V. Pop, Proc. Int. Conf. Powder Metall., Sinaia, Romania, 2005, vol. 2 , p. 887.
[133] F. Popa, O. Isnard, I. Chicinaş, V. Pop, J. Magn. Magn. Mater. (2007), accepted.
[134] M. Manivel Raja, K. Chattopadhyay, B. Majumdar, A. Narayanasamy, J. Alloys Comp. **297**, 199 (2000).
[135] S.W. Mahon, R.F. Cochrane, M.A. Howson, Nanostruct. Mater. **7**, 195 (1996).
[136] Y.Q. Zhang, Z.D. Zhang, Q.F. Xiao, D.I. Geng, X.G. Zhao, W.S. Zhang, C.Y. You, J. Phys. D: Appl. Phys. **36**, 1159 (2003).
[137] L. C. C. M. Nagamine, A. Chamberod, P. Auric, S. Auffret, L. Chaffron, J. Magn. Magn. Mater. **174**, 309 (1997).
[138] T. D. Shen, R. B. Schwarz, J. D. Thompson, Phys.Rev B **72**, 014431-1 (2005).
[139] I. Chicinas, O. Isnard, O. Geoffroy, V. Pop, Proc. World Congress Powder Metall., Vienna, Austria, **4**, 623. (2004).
[140] I. Chicinas, O. Geoffroy, O. Isnard, V. Pop, J. Magn. Magn. Mater. **290-291**, 1531 (2005).
[141] I. Chicinas, O. Geoffroy, O. Isnard, V. Pop, J. Magn. Magn. Mater. **310**, (2007) 2474.
[142] L. Schultz, K. Schnitzke, J. Wecker, M. Katter, C. Kuhrt, J. Appl. Phys. **70**, 6339 (1991).
[143] P. A. P. Wendhausen, B. Gebel, D. Eckert, K. H. Muller, J. Appl. Phys. **75**, 6019 (1994).
[144] M. Venkatesan, C. Jiang, J. M. D. Coey, J. Magn. Magn. Mater. **242-245**, 1350 (2002).
[145] K. O'Donnell, J. M. D. Coey, J. Appl. Phys. **81**, 6311 (1997).
[146] L. Wei, W. Qun, X. K. Sun, Z. Xin-guo, Z. Tong, Z. Zhi-dong, Y. C. Chuang, J. Magn. Magn. Mater. **131**, 413 (1994).
[147] J. X. Zhang, L. Bessais, C. Djega-Mariadassou, E. Leroy, A. Percheron-Guegan, Y. Champion, Appl. Phys. Lett. **80**, 1960 (2002).
[148] D. L. Leslie-Pelecky, R. L. Schalek, Phys. Rev. **B59**, 457 (1999).
[149] D. Geng, Z. Zhang, B. Cui, Z. Guo, W. Liu, X. Zhao, T. Zhao, J. Liu, J. Alloys and Compounds **291**, 276 (1999).
[150] C. Djega-Mariadassou, L. Bessais, J. Magn. Magn. Mater. **210**, 81 (2000).
[151] A. Nandra, L. Bessais, C. Djega-Mariadasssou, E. Burzo, J. Magn. Magn. Mat. **272-276**, 1243 (2004)
[152] D. Geng, Z. Zhang, B. Cui, W. Liu, X. Zhao, M. Yu, J. Magn. Magn. Mater. **224**, 33 (2001).
[153] Z. Chen, Y. Zhang, G. C. Hadjipanayis, J. Magn. Magn. Mater. **219**, 178 (2000).
[154] C. You, X. K. Sun, W. Liu, B. Cui, X. Zhao, Z. Zhang, J. Phys. D.: Appl. Phys. **33**, 926 (2000).
[155] W. Liu, Z. D. Zhang, J. P. Liu, X. K. Sun, D. J. Sellmyer, X. G. Shao, J. Magn. Magn. Mater. **221**, 278 (2000).
[156] R. Grossinger and Reiko Sato, , J. Magn. Magn. Mater. **294**, 91 (2005).
[157] M.A. Al-Khafaji, W.M. Rainforth, M.R.J. Gibbs, H.A. Davies, J.E.L. Bishop, J. Magn. Magn. Mater. **188**, 109 (1998).
[159] V. Neu, L. Schultz, J. Appl. Phys. **90**, 1540 (2001)
[160] A. Bollero, A. Yan, O. Gutfleisch, K.H. Muller, L. Schultz, IEEE Trans Magn. **39**, 2944 (2003)
[161] V. Pop, O. Isnard, I. Chicinas, D. Givord, Proc. Euro PM2005 Congress, Prague 2005, Vol.1, p. 445 .

[162] V. Pop, O. Isnard, I. Chicinas, D. Givord, J.M. Le Breton, J. Optoelectron. Adv. Mater., **8**, 494 (2006).
[163] V. Pop, O. Isnard, I. Chicinaş, D. Givord, J. Magn. Magn. Mater. (2007) in press.
[164] D.Givord, O. Isnard, V. Pop, I. Chicinaş**,** J. Magn. Magn. Mater. (2007) accepted.
[165] E. Lectard, C. H. Allibert, R. Ballou, J. Appl. Phys. **75,** 6277 (1994).
[166] E. Dorolti, V. Pop, O. Isnard, D. Givord, I. Chicinaş J. Optoelectron. Adv. Mater. **9** (2007), in press.
[167] B.M. Ma, J.W. Herchenroeder, B. Smith, M. Suda, D.N. Brown, Z. Chen, J. Magn. Magn. Mater. **219**, 418 (2002).
[168] X. Rui, J.E. Shield, Z. Sun, L. Yue, Y. Xu, D.J. Sellmyer, Z. Liu, D.J. Miller, J. Magn. Magn. Mater. **200,** 73 (1999).

*Corresponding author: viorel@phys.ubbcluj.ro